Розглянуто удосконалення контуру регулювання струму багатофункціонального мережевого інвертора системи електроживлення локального об'єкту. Метою дослідження є забезпечення відповідності стандартам якості струму мережі у всьому діапазоні його значень для спільної точки підключення навантаження, розподільчої мережі змінного струму і перетворювального агрегату фотоелектричної системи. Запропоновано використання релейного регулювання струму з комбінуванням уніполярної і біполярної модуляції в поєднанні з модифікованим алгоритмом перемикання ключів інвертора. Показано, що за нелінійного навантаження стрибкоподібна зміна похідної завдання струму інвертора призводить до різкої зміни частоти перемикання ключів. Це спричиняє появу «сплеску» у струмі мережі, що погіршує його гармонійний склад за малих значень.

За нелінійного реактору зі збільшенням струму інвертора «сплеск» також обумовлено змінюванням частоти перемикання ключів. Це відбувається на ділянках зростання (спадання) струму внаслідок змінювання індуктивності реактора. Встановлена залежність заданого відхилення для релейного регулятора, що за лінійного реактору забезпечує практично постійну частоту перемикання ключів інвертора. Запропоновано враховувати похідну сигналу завдання струму інвертора при формуванні значень відхилень релейного регулятора, що дозволить виключити стрибкоподібне змінювання частоти перемикання ключів. Показана необхідність врахування несинусоїдальності напруги мережі при визначенні напруги на вході інвертора. Запропоновано зменшення ємності конденсатору фільтру в спільній точці підключення та використання зв'язку за струмом конденсатору. За несинусоїдальної напруги мережі це сприятиме покращенню якості струму мережі. Запропоновано структуру контуру регулювання струму з релейним регулятором струму за комбінованою модуляцією та регулюванням заданого значення відхилення регулятору. Регулювання здійснюється згідно з заданим значенням амплітуди і похідної струму інвертора. Розроблено математичну модель системи «мережа – мережевий інвертор – навантаження» з блоком визначення втрат потужності в ключах і нелінійним реактором

Ключові слова: релейний регулятор струму, уніполярна та біполярна модуляція, втрати потужності, коефіцієнт гармонік, моделювання системи

UDC 620. 92 : 621.314/. 572
DOI: 10.15587/1729-4061.2019.185391

IMPROVEMENT OF THE CURRENT CONTROL LOOP OF THE SINGLE-PHASE MULTIFUNCTIONAL GRID-TIED INVERTER OF PHOTOVOLTAIC SYSTEM

A. Shavelkin
Doctor of Technical Sciences, Professor*
E-mail: shavolkin@gmail.com
Jasim Mohmed Jasim Jasim
PhD, Associate Professor
Department of Electrical Power Engineering Techniques
Al-Furat Al-Awsat Technical University
Al-Musssaib Technical college
Al-Najaf Baghdad main road, 15,
Al-Kufa, Iraq, 54001
E-mail: jm.jasem@atu.edu.iq
I. Shvedchykova
Doctor of Technical Sciences, Professor*
E-mail: ishved@i.ua
*Department of Energy Management and Applied Electronic Engineering
Kyiv National University of Technologies and Design
Nemyrovycha-Danchenka str., 2
Kyiv, Ukraine, 01011

Received date 30.08.2019
Accepted date 17.11.2019
Published date 21.12.2019

1. Introduction

In combined electric power systems (EPS) of local objects with renewable energy sources (RES), the load of the object is connected to the point of common coupling (PCC) of 0.4 kV AC distributed grid (DG) and RES converter unit (CU). In the case of photovoltaic solar battery (PV), the utilization factor of the quite expensive CU equipment is no more 20 % [1]. More time this equipment is not used or not fully used. A promising direction is the use of a multifunctional grid voltage source inverter (VSI) that combines the functions of an active power filter (APF) [2]. This contributes to increasing the utilization factor of CU due to its round-the-clock use [2–5] to maintain the maximum (close to one) power factor at the PCC to DG. The result is reduced load and energy loss in the DG. It is also possible to provide an autonomous mode of operation during the daytime [2, 3], stabilization of the load voltage [4]. Thus, improving the indicators of CU for systems with RES is an urgent task and contributes to the further development of energy with distributed sources of electricity.

2. Literature review and problem statement

The quality of the current generated at the PCC is determined by the VSI current control loop (CCL) and its output LC or LCL filter. The filter provides suppression of the higher harmonics. The decisive role in suppressing the high harmonics of the low order generated by the load is played by CCL. In [2], a review of circuit designs and control structures of the VSI is performed. It follows that the main types of CCL structures are based on the use of a proportional-integral (PI) controller, a relay current controller (RCC), and a sliding mode. In [5], for a three-phase VSI, a solution with a controller based on fuzzy logic is presented.

Compared to generating VSI [6], which operate on a DG and form a sinusoidal current with a THD <3.5 %, in EPS of the local object with a nonlinear load, the current of the multifunctional grid VSI is non-sinusoidal. In this case, VSI compensates higher harmonics of low order of load current. The modulation components of VSI current are suppressed by the output filter and grid current at PCC is almost sinusoidal. The presence of error in the process of CCL current formation leads to distortion of generated grid current. The error causes the presence of higher harmonics of low order in the current (3rd, 5th, ...). This complicates the issue of ensuring the conformity of the harmonic composition of grid current to IEC standards [7, 8].

PWM solutions are more common because the modulation frequency is constant. So, in [9, 10], the deviation of i_C current relative to the reference value i_C^* $\left(\Delta i_C = i_C^* - i_C\right)$ is given through the PI current controller. However, its efficiency in eliminating errors even at a modulation frequency of 20 kHz is insufficient, as evidenced by the oscillograms given in [9, 10]. In [2], variants of CCL are considered, in which a voltage proportional to the voltage of the DG is added to the output voltage of the current controller. Also in [2], options are considered with the addition of voltages proportional to i_C^*, i_C and grid voltage u_g to the output of the current controller. However, these solutions are effective only at a sufficiently high modulation frequency. For example, in [6], during the use of PI controller in CCL at a PWM frequency of 20 kHz, the value of THD for grid current (THDi_g) is 4.8 % at the current amplitude I_{gm}=10 A (amplitude of VSI current is 20 A, nonlinear load is 9 A). However, the possibilities of increasing the modulation frequency are limited, as this will lead to increased power losses in VSI switches and reducing its efficiency. The same applies to the use of the sliding mode [11, 12], when the modulation frequency is 90 kHz. Acceptable indicators for a modulation frequency of 6.8 kHz provide a rather complicated option in the implementation of CCL using dynamic error compensation [13].

The option of overcoming the corresponding difficulties may be the use of RCC, which eliminates the error of VSI current formation and provides a high speed of CCL. However, the switching frequency f_S of VSI switches is variable. This can provoke oscillations in the output filter and leads to a "splash" in DG current [5], which worsens its harmonics composition. Decisions on RCC [2, 14] refer to the use of bipolar voltage modulation for VSI bridge circuits, when the output voltage u_C takes two values (U, $-U$). In this case, f_S is twice as large as for unipolar modulation. There are attempts to solve the question of frequency stabilization. So, in [15], unipolar modulation with a constant frequency f_S with three voltage levels u_C (U, 0, $-U$) is considered, but for RL loads in the absence of connection to the DG. In case of parallel work with DG, the application of state u_C=0 in certain intervals of time does not provide the required law of VSI current change and is quite problematic. A solution with a combination of unipolar and bipolar modulation [16] looks promising, but it does not provide for stabilization of f_S.

Generally, the dependence of inductance of the VSI output reactor on current is not taken into account when setting the CCL. However, the change of inductance value can be quite large – several times, which will affect the CCL functioning. In [17], a solution is considered with the regulation of the grid current using a nonlinear reactor and a PWM frequency of 20 kHz. In this case, the VSI current and load current are calculated using a self-learning algorithm.

In the considered solutions, the operation of the VSI on a DG with a sinusoidal voltage is considered. In [18], an assessment is made of the effect of the higher harmonics of the DG voltage on the harmonic composition of current for the generating VSI without taking into account the load. At the same time, the standard [19] admits non-sinusoidal voltage for the grid (public electricity networks). Allowable relative (to the main harmonic) values of higher harmonics of voltage are normalized. Naturally, the current of the load for this case will also be non-sinusoidal. These harmonics of current will be compensated by the grid VSI. The question of the influence of non-sinusoidal DG voltage on the possibilities of VSI current formation without error arises, which requires a certain rate of VSI current change and corresponding determination of the parameters of its circuit. In the presence of filter capacitor at PCC to DG, there is a question regarding the higher harmonics of the capacitor current in case of the non-sinusoidal voltage of DG.

So, in [13], the capacitor capacitance is C=60 μF, respectively, the amplitude of the first harmonic $I_{fm(1)}$=5.88 A. For example, in the case the relative value of the 13th harmonic of DG voltage is 3 %, the value is $I_{fm(13)}$=13·0.03$I_{fm(1)}$= 2.29 A. If the value of sinusoidal current consumed from DG (or generated to DG) I_{gm}=2÷10 A, then it is impossible to obtain an acceptable value of THDi_g≤5 %. Limiting the values of current higher harmonics that are added by the capacitor to the current generated by CU at PCC to DG requires additional research.

So, the issue of LCC implementation for grid-tied VSI is insufficiently studied and requires additional research. Improvement of the system with RCC is promising, because error absence in the process of VSI current formation creates conditions for improving the harmonic composition of DG current at its small values.

3. The aim and objectives of the study

The aim of the study is to ensure THD≤5 % for the grid current in the entire range of its values when using a multifunctional grid VSI. This is achieved by improving CCL with a relay controller.

To achieve this aim, the following objectives are accomplished:

– to study the mechanism of VSI current formation for parallel operation with the DG and non-linear load. To study the possibilities of improving the principles of relay control of current with combining unipolar and bipolar modulation for using a linear and non-linear output reactor of VSI;

– to study the possibilities of ensuring current quality in PCC at the non-sinusoidal voltage of DG;

– to develop an appropriate VSI control system structure;

– to develop a mathematical model of the system "DG – grid VSI – load" to verify the effectiveness of the solutions. This will also expand the possibilities of studying processes in the circuits.

4. Investigation of the mechanism of current formation and implementation of the CCL of the grid VSI with combined modulation

4. 1. Structure of the power circuits and determination of parameters of single-phase EPS

The structure of single-phase EPS (Fig. 1) consists of the grid VSI with the bridge circuit with the output reactor or two reactors in every VSI output with total inductance L.

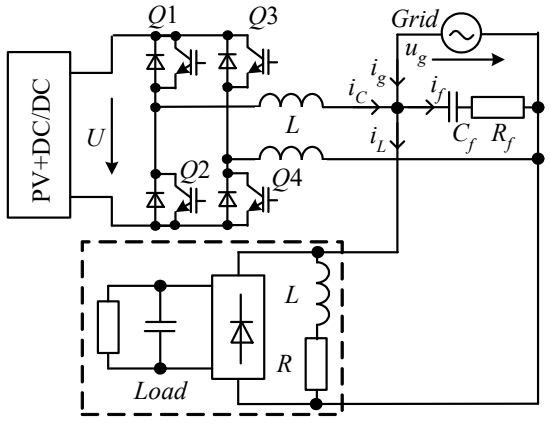

Fig. 1. Structure of CU power circuits

VSI and load are connected to DG with voltage $u_g=U_{gm}\sin\omega t$ (U_{gm} – voltage amplitude, $\omega=2\pi f$ – angular frequency, f=50 Hz). The load is active-inductive and non-linear (unmanageable rectifier). Capacitor filter (C_f with small R_f) ensures the suppression of higher harmonics in PCC to DG. In fact, we have an LC-filter and taking into account the DG inductance L_g it is actually an LCL-filter. The resistor R_f in the condenser circuit reduces the Q-factor of the filter (decreasing the oscillation). A solar battery (PV) with a voltage converter (DC/DC) is connected to the VSI DC link. DC/DC supports a reference value of voltage U at the VSI input.

In the current source mode of VSI, when operating in parallel with DG, it is necessary that $U=aU_{gm}$ ($a>1$) [12, 13]. The rate of changes (derivative) in the VSI output current $\mathrm{d}i_C/\mathrm{d}t$ in this case must exceed the maximum value of the derivative of the current reference $\mathrm{d}i_C^*/\mathrm{d}t$.

In the case of sinusoidal current formation, the maximum value of the derivative of the current reference is $\left(\mathrm{d}i_C^*/\mathrm{d}t\right)_{\mathrm{MAX}}=\omega I_{Cm\mathrm{MAX}}$ ($I_{Cm\mathrm{MAX}}$ – amplitude for the maximum value of VSI current). We consider the value of the inductance L of the output reactor constant. Then, $\mathrm{d}i_C/\mathrm{d}t$ can be determined in accordance with the value of the voltage of the VSI output reactor

$$u_L=u_g-u=L\frac{\mathrm{d}i_C}{\mathrm{d}t}. \quad (1)$$

The smallest value u_L takes the place when $u_g=U_{gm}$, then

$$U_L=U-U_{gm}=L\omega I_{Cm\mathrm{MAX}}.$$

Hence

$$a>1+\frac{L\omega\cdot I_{Cm\mathrm{MAX}}}{U_{gm}}.$$

When VSI is combined with APF function and the nonlinear load is used, VSI current shape is distorted with an abrupt change $\mathrm{d}i_C/\mathrm{d}t$. Consequently, the a value will determine the possibility of providing the maximum value $(\mathrm{d}i_C/\mathrm{d}t)_{\mathrm{MAX}}$ in the process of current formation without error. In this case, the minimum value is

$$\left(\frac{\mathrm{d}i_C}{\mathrm{d}t}\right)_{\mathrm{MIN}}=\frac{(a-1)U_{gm}}{L},$$

and the maximum (at u_g=0) value is

$$\left(\frac{\mathrm{d}i_C}{\mathrm{d}t}\right)_{\mathrm{MAX}}=\frac{aU_{gm}}{L}.$$

Relative to DG voltage, the value of the reactor voltage U_L (in the first harmonic) for the maximum VSI current $I_{C\mathrm{MAX}}$ (RMS value) is $b=\frac{U_L}{U_g}=\frac{\omega L\cdot I_{C\mathrm{MAX}}}{U_g}$ (U_g – RMS value of DG voltage). The inductance of the VSI reactor, based on this

$$L=\frac{bU_{gm}}{\omega\sqrt{2}I_{Cm\mathrm{MAX}}}. \quad (2)$$

Thus, $a>1+nb$ and it determines $\mathrm{d}i_C/\mathrm{d}t$.

4. 2. Using a relay current controller at combined modulation of the VSI output voltage

In spite of the perturbation character, RCC eliminates the current formation error in case of ensuring a sufficient rate of VSI current change.

The grid voltage u_g and output VSI current i_C are shifted by the phase at the angle θ. So we have intervals where the polarities u_g and i_C coincide. In case of unipolar modulation, the formation of current at these intervals is problematic, since shorting of the inverter output circuit through open switches at the output voltage of VSI u_C=0 does not provide the required value $\mathrm{d}i_C/\mathrm{d}t$. In this case, there is a need to change the voltage polarity of VSI. In case of using RCC, this involves the use of additional switching levels, but does not preclude current distortion.

The combined principle of VSI current formation [16] with the transition from unipolar to bipolar modulation allows solving this problem. Bipolar modulation is carried out in a zone of angles symmetric with respect to the point of polarity change u_g up to 30° at small values of the VSI current. Consequently, this will not lead to a significant increase in energy losses in VSI switches.

4. 3. RCC parameters determination

We consider the possibility of RCC implementation with a constant switching frequency of switches f_S. We assume that the inductance of the reactor is constant. The process of VSI current i_C formation for unipolar modulation is illustrated in Fig. 2.

For simplicity, we assume that the reference value of the current VSI i_C^* at a certain time interval is constant. Switching the VSI state is carried out upon reaching the current deviation $|\Delta i_C| \geq \delta$ (δ – given deviation value). The amplitude of current pulsations $\delta = \Delta I_{Cm} = \Delta I_C/2$ relative to the given value is determined by the duty ratio of VSI voltage pulses $\gamma = t_{on}/T$ (t_{on} – switch-on time, T – switching period).

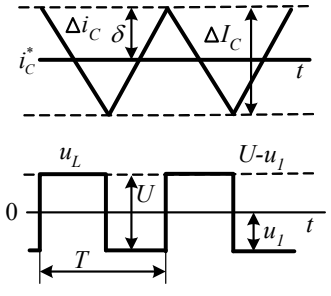

Fig. 2. RCC operation at unipolar modulation

The dependences $\gamma(t)$ and $\Delta I_{Cm}(t)$ can be determined under the condition $\int_0 u_L \mathrm{d}t = 0$. So, for $u_C > 0$ we have

$$U_{gm}(a - \sin\omega t)\gamma + U_{gm}(0 - \sin\omega t)(1-\gamma) = 0.$$

Hence $\gamma = \dfrac{\sin\omega t}{a}$.

The amplitude of current deviation

$$\Delta I_{Cm} = \frac{\gamma(1-\gamma)aU_{gm}}{2Lf_s}.$$

Taking into account the value γ, we obtain

$$\Delta I_{Cm}(t) = \frac{U_{gm}}{a \cdot 2Lf_s} \times$$
$$\times (a\sin\omega t - 0.5 + 0.5\cos 2\omega t).$$

For a negative half-wave of VSI voltage $u_C < 0$, we have a similar picture. According to this, in the general case, we obtain

$$\delta = \Delta I_{Cm}(t) =$$
$$= \frac{U_{gm}}{a \cdot 2Lf_s}(|a\sin\omega t| - 0.5 + 0.5\cos 2\omega t) =$$
$$= \frac{U_{gm}}{a \cdot 2Lf_s} A(t). \qquad (3)$$

Similarly, during bipolar modulation it is possible to determine the dependence $\delta(t)$ when u_C takes the values U and $-U$

$$\delta_2(t) = \frac{aU_{1m}}{4Lf_s}\frac{(a^2 - \sin^2\omega t)}{a^2}.$$

Taking into account that bipolar modulation is carried out in a narrow area, when the value $\delta_2(t)$ is close to maximum, it will be enough to use its fixed value.

Compared to unipolar PWM, the use of RCC has features, since the switching frequency of switches corresponds to the switching frequency of the controller f_S.

For the same value of equivalent modulation frequency of VSI voltage, the value of switching frequency of switches is twice as high as when using PWM. This necessitates taking into account the energy losses in the switches of the VSI. Reducing the number of switching steps of VSI switches can be achieved when control pulses ($g_1 \div g_4$) are divided for switches $Q1 \div Q4$ according to the output voltage of RCC u_{hR} as follows:

$$u_R = u_{hR} \cdot sign(i_c^*),$$

$$g_1 = 1, \text{ if } u_R \geq 0 \text{ and } g_1 = 0, \text{ if } u_R < 0;$$

$$g_3 = 1, \text{ if } u_R \leq 0 \text{ and } g_3 = 0, \text{ if } u_R > 0;$$

$$g_2 = \overline{g}_1, \quad g_4 = \overline{g}_3.$$

During the half-period, one of VSI switches is on, for example, when $di_C^* > 0$ the switch $Q1$ is on and switches $Q3$, $Q4$ are switched. Accordingly, the number of switching steps of switches during the period is twice less than the switching frequency of RCC. To evenly load switches by current, it is necessary to periodically change the order of switching of switches $Q1$ to $Q4$, $Q3$ to $Q2$.

The relay method of current formation is dependent on the rate of changes in the reference current. So, in the presence of diode rectifier in the load, its current that is consumed from DG has a pulsed character and the derivative of current during switching of diodes changes abruptly. The VSI reference current has the same character (Fig. 3). At sufficient for forming i_C^*, but limited value $\mathrm{d}i_C/\mathrm{d}t$ and an abrupt change of the value $\mathrm{d}i_C^*/\mathrm{d}t$ the frequency of RCC switching sharply decreases (Fig. 3 shows that the switching period of RCC T_1 in comparison with T is almost doubled). This leads to a "splash" in the grid current.

The "splash" suppression is possible by a general increase of frequency f_S in the case of δ decrease in accordance with (1) with a constant voltage $U(a)$, but due to increased power losses in VSI switches, the possibilities of this are limited.

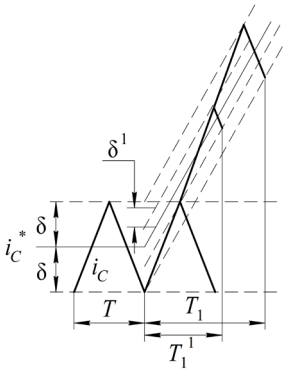

Fig. 3. Change of VSI current reference derivative

To reduce the effect of changes in the value $\mathrm{d}i_C^*/\mathrm{d}t$ on the switching frequency of RCC, it is necessary to increase $\mathrm{d}i_C/\mathrm{d}t$, which is achieved by increasing $U(a)$. From the geometric relations from Fig. 3 it is not difficult to show that the relative increment time to the moment when current reaches a reference deviation δ decreases with increasing $\mathrm{d}i_C/\mathrm{d}t$. Accordingly, when the value $\mathrm{d}i_C^*/\mathrm{d}t$ is constant, the relative value of changes in the switching period (frequency) and "splash" in the grid current decrease.

An effective means of equalizing the switching frequency of the RRC is the change of the reference deviation δ according to $\mathrm{d}i_C^*/\mathrm{d}t$. Further, this is defined as Dynamic Compensation (DK). So with an increase in the derivative $\mathrm{d}i_C^*/\mathrm{d}t$, the value of δ (δ¹ in Fig. 3) is reduced with the corresponding increase and alignment of the switching frequency value (in Fig. 3, the value of $T_1^1 \approx T_1$).

The implementation of the scheme with the nonlinear reactor, when its inductance changes according to VSI current and decreases with increasing of its value has some features.

In the general case, L can change several times. According to (1), this leads to an increase of $\mathrm{d}i_C/\mathrm{d}t$ and an increase of RCC switching frequency. As a result, at significant amplitudes of i_C, the effect of changes in the derivative $\mathrm{d}i_C^*/\mathrm{d}t$ on switching frequency decreases. In the area where current values i_C are close to maximum, we receive significant energy losses in VSI switches. To reduce them, it is necessary to reduce frequency f_S (increase δ). In case of decreasing current and increasing L, f_S decreases significantly. So, there is another factor for the appearance of "splash" in the grid current. Control δ when the reactor is nonlinear does not provide a constant switching frequency of VSI switches, but contributes to the alignment of its value and "splash" suppression. Therefore, it is advisable to regulate the deviation δ according to the amplitude i_C^*.

4. 4. Structure of the control system

CCL structure (Fig. 4) consists of: adder devices; multiplier blocks; block of phase locked loop PLL; relay element RE; converter C of unipolar RE signal in bipolar. The following are also used: pulse generator-distributor unit F; functional converter FC, which forms the reference value of deviation δ according to the amplitude value i_C^* and sets the modulation mode; dynamic compensation unit DK, which performs a change in the value of δ in accordance with the derivative i_C^*.

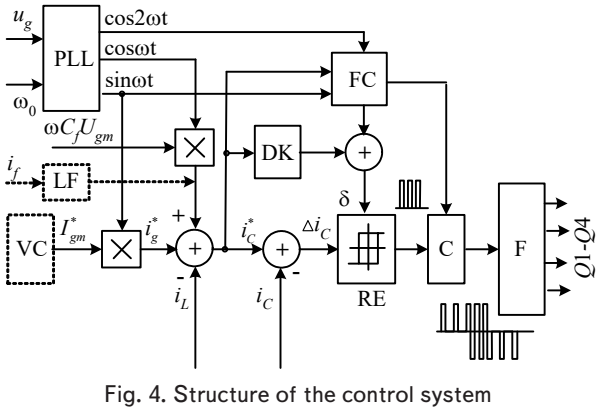

Fig. 4. Structure of the control system

The reference signal for the amplitude of the grid current I_{gm}^* is formed by an external voltage controller VC, which maintains the voltage at the VSI input at a given level $U=U^*$. In accordance with I_{gm}^*, a sinusoidal signal of reference of the grid current i_g^* is formed. It, when generating the energy of the SB to the grid, is shifted relative to voltage ug by 180°, and in the case of energy consumption from the grid it coincides in phase. Reference of the grid VSI current is determined with taking into account the load current i_L and calculated value of the capacitive component (first harmonic) of the filter current with the amplitude $I_{fm(1)}=\omega C_f U_{gm}$. This variant can also be used in the case of the non-sinusoidal voltage of the DG.

Fig. 4 also shows a variant with using the signal of the filter capacitor current (shown by dotted lines). For this, the signal from the current sensor is fed through the filter LF. The calculated value $i_f=C\mathrm{d}u_g/\mathrm{d}t$ can also be used. Using the LF filter is necessary to suppress the modulation harmonics of the current. This solution in the case of non-sinusoidal DG voltage creates certain possibilities for compensating the higher harmonics of the capacitor current by VSI. This is done the same as for the load current harmonics, and provides an improvement in the harmonic composition of the DG current. These possibilities are limited due to the phase shift of higher harmonics at the LF output and relate to the 3rd and 5th harmonics of low order for which the phase shift is minimal.

PLL forms signals $\sin\omega t$, $\cos\omega t$, $\cos 2\omega t$ according to the DG voltage $u_g=U_{gm}\sin\omega t$ and given value of angular frequency ω_0.

4. 5. Simulation in Matlab and its results

The simulation was carried out according to the structures in Fig. 1, 4 with combining the constant non-linear load (unmanaged rectifier with output capacitive filter and load power 900 W) and *RL* load.

VSI power supply was carried out from a DC source of constant voltage. General load power is P_L=2745 W, it's 0.5 of the maximum VSI power at $I_{Lm(1)}$=19.8 A, $\phi_{(1)}$=27°. DG model (220 V, f=50 Hz) consists of resistance R=0.02 Ohm, X_{Lg}=0.02 Ohm. Filter parameters are R_f=0.3 Ohm, C_f=60 μF. Grid VSI with $I_{C\mathrm{MAX}}$=25 A ($I_{Cm\mathrm{MAX}}$=35.35 A). In the case of non-sinusoidal DG voltage, a serial connection of the AC voltage sources with the corresponding frequency and amplitude values is used. The use of a linear reactor with R=0.1 Ohm and L=0.0042 H (b=0.15) and a nonlinear reactor with the same initial parameters is considered.

A block of power losses determinations in the switches was used to estimate the efficiency of the considered [21] solutions. According to the parameters of the VSI model, the use of IGBT module SK 25 GH 12T4 was reviewed [20]. Losses of power of conduction P_C and switching P_{SW} were taken into account. In this case, $P_C=\frac{1}{T}\int_0^T u_V i_V \mathrm{d}t$ (u_V, i_V – instantaneous values of the voltage and current of the switches (diode and transistor), T – period of the output frequency). The value of i_V is determined in the VSI model, u_V is determined for i_V in accordance with the volt-ampere characteristic of the switches. P_{SW} values are determined from the switching energy dependencies [20] $E_{on}=f(i_{Von})$, $E_{off}=f(i_{Voff})$ for the transistor and E_{rr} – for the diode according to the i_V value at the moment of switches switching. Energy values are given at the standard voltage value U_{CT} (U_{CT}=600 V for the voltage class 1200 V) and temperature T_j=150 °C.

For temperature values lower than T_j, the energy losses are reduced, so the temperature was not taken into account for simplification. The dependence $E'=E\left(\frac{U}{U_{CT}}\right)^{K_V}$ (K_V=1.35 for IGBT and K_V=0.6 for the diode) is used to recalculate to the actual value of VSI voltage U.

The current values of the switches i_{Von} and i_{Voff} are determined according to the forward and back fronts of the current pulses. The integrator is used as a sample and hold circuit with accumulation to sum up switching energy values. Measurement is carried out with averaging over 4 periods of DG voltage.

The model of nonlinear reactor which inductance is dependent on current. In the SimPowerSystems library, the element with controlled inductance value is absent. Therefore, the standard model of the transformer with the non-linear characteristic of the magnetic circuit (Saturable transformer) was used. This characteristic is given in a table (piecewise-linear) form corresponding to the current value. The primary transformer winding was used as the reactor. In advance, before using in the general model, separate studies were carried out to verify the correctness of obtaining the given values of inductance (from 0.0042 H to 0.00158 H) in the operating range of currents. In this case, the primary winding was connected to the pulsed DC source and its current was measured. The inductance value was determined in accordance with the rate of current change in the interval of connecting the reactor to the source.

All comparisons of indicators were carried out for the same load and close values of THDi_g in the range of the given DG current values I^*_{gm} =2–17.8 A (17.8 A corresponds to the maximum value of the amplitude of the VSI current fundamental harmonic). The work of the system with sinusoidal and non-sinusoidal DG voltage is considered.

Sinusoidal DG voltage. Linear reactor with L=0.0042 H. Voltage values at the VSI input (U) with a=1.3. The influence of the law of changes in the given deviation value δ is estimated. Four variants of control are presented:

1 – δ=const;

2 – δ changes according to (3);

3 – δ=const with the use of dynamic compensation;

4 – δ changes according to (3) with the use of dynamic compensation.

Variants 3 and 4 ensure minimum energy losses in the switches when they have close values. When THDi_g values are close, variant 4 allows reducing power losses in the VSI switches by 35 % at a current $I^*_{gm}=2$ A (THDi_g=4.1 %, efficiency η=0.976 is determined taking into account energy losses in the VSI switches) and 25 % at a current $I^*_{gm}=17.8$ A (THDi_g=0.68 %, η=0.977).

Non-linear reactor. Compared to L=const, we have a general increase in energy losses up to 15 %. DK influence is reduced and for the current $I^*_{gm}=2$ A losses decrease to 22 %. However, the efficiency remains valid. So, at $I^*_{gm}=3$ A and $I_{Lm(1)}$=14.8 A (THDi_g=3.36 %), the efficiency is 0.977. When the load increases at $I^*_{gm}=3$ A and $I_{Lm(1)}$=19.8 A (THDi_g=3.36 %), the efficiency is 0.974. Oscilograms of u_g, u_C voltages, i_g, i_C, i_L currents and $\left(\mathrm{d}i^*_C/\mathrm{d}t\right)\cdot 10^4$ for variant 3 at $I^*_{gm}=2$ A and THDi_g=4.1 % are presented in Fig. 5. Fig. 6 shows the current spectrum in the case of DK disconnection under the same conditions – THDi_g=9.2 %.

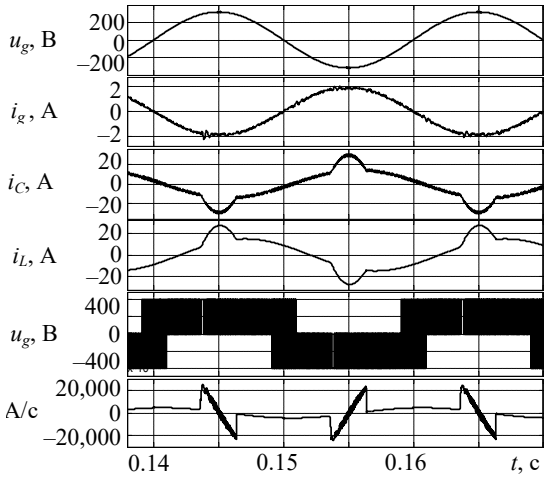

Fig. 5. Oscillograms u_g, u_C, i_g, i_C, i_L for variant 3

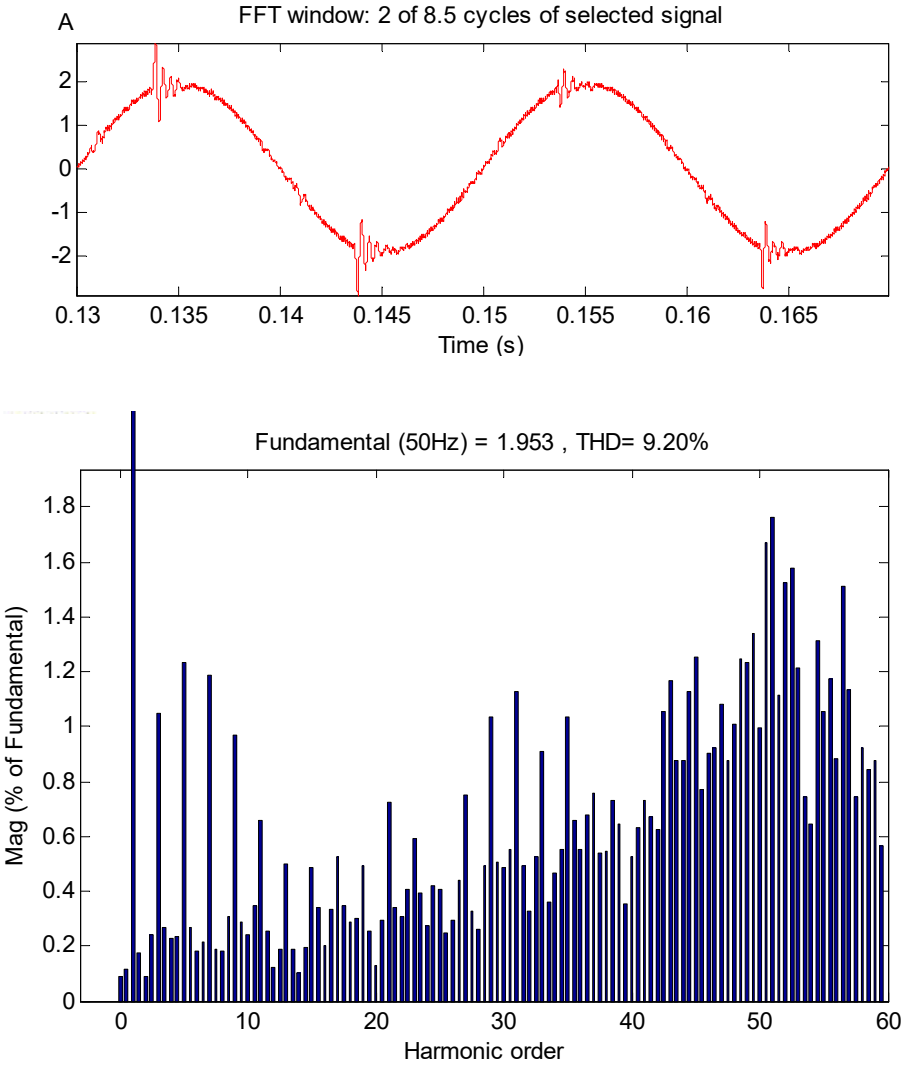

Fig. 6. Oscillogram and i_g spectrum in the DK absence

In the case of a non-linear reactor, the nature of the "splash" processes somewhat varies. The effect of DK and setting the δ value according to (3) are significant only in the initial part of the reactor characteristic $L(I_C)$ with $I_C \approx 0.5 I_{CMAX}$. So at $I^*_{gm}=10$ A in comparison with δ=const (in Fig. 7 we have a "side splash"), this allows virtually eliminating the

"splash" and reducing the loss of switches by 9 %. As the VSI current amplitude increases, the rate of current change and, accordingly, the switching frequency increase due to a decrease in reactor inductance. In this case, DK is not needed and leads to an increase in power losses.

In this case, the goal is to reduce the switching frequency of the switches, when the values of i_C^* are close to the maximum, as well as to equalize the switching frequency when switching to the linear section $L(I_C)$. The system is stable in dynamics, as shown by the oscillograms u_g, u_C, i_g, i_C, i_L, $\left(\mathrm{d}i_C^*/\mathrm{d}t\right)10^{-3}$ (Fig. 8) in case of a decrease in RL load at the time t=0.145 s at a constant value of current $I_{gm}^* = 5$ A.

Non-sinusoidal DG voltage. Table 1 shows the relative values of the maximum rate of change of the reference current $\left(\mathrm{d}i_C^*/\mathrm{d}t\right)^*$ when individual harmonics are added to the DG voltage with a ratio of n to the main frequency and all of them simultaneously (all). Values are given relative to the value of $\mathrm{d}i_C^*/\mathrm{d}t = 29000$ A/c (at given load parameters) at a sinusoidal DG voltage (n=1). On the other hand, the standard [15] restricts the total value of voltage THDu_g at 8 %.

Then proceeding from the fact that $\left(\frac{\mathrm{d}i_C}{\mathrm{d}t}\right)_{MIN} = \frac{(a-1)U_{gm}}{L}$, a=1.6 (U=500 V) can be considered sufficient.

Table 1

Relative value of the maximum rate of VSI reference current change

n	1	3	5	7	9	11	13	All
$\left(\mathrm{d}i_C^*/\mathrm{d}t\right)^*$, p.u.	1	0.82	1.5	1.41	0.93	1.59	1.26	2.24

Capacity C_f and resistance R_f. The value of the filter capacitor capacitance is halved to 30 μF. This allows at sinusoidal DG voltage and U=500 V obtaining THDi_g=4.22 % at $I_{gm}^* = 3$ A. In the case of introducing the coupling on the current i_{Cf} into the channel forming the VSI current reference, the exclusion of the modulation current components is ensured by the resistance value R_f=0.8 Ohm in combination with the LF filter with a time constant of $4{\cdot}10^{-4}$ s. In this case, the system is resistant to disturbances.

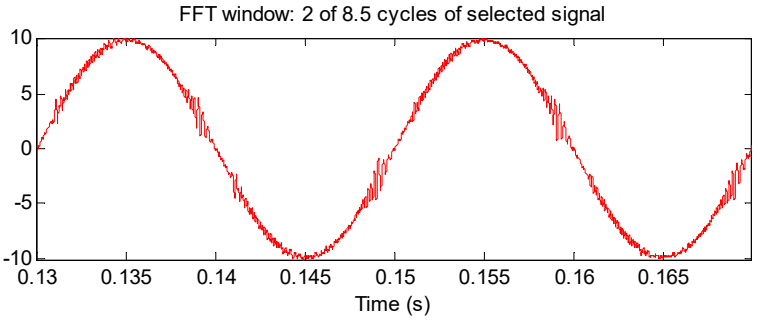

Fig. 7. "Side splashes" of i_g current when using a nonlinear reactor and δ=const

The best indicators when using i_{Cf} current coupling to compensate for the effect of the non-sinusoidal voltage of the DG is achieved in the case of setting the value δ according to (3) in combination with DK. In Table 2, THDi_g values are given in the presence of harmonic with order n in the DG voltage in the case of using i_{Cf} current coupling for the minimum values of I_{gm}^*, when THDi_g≤5 % is provided.

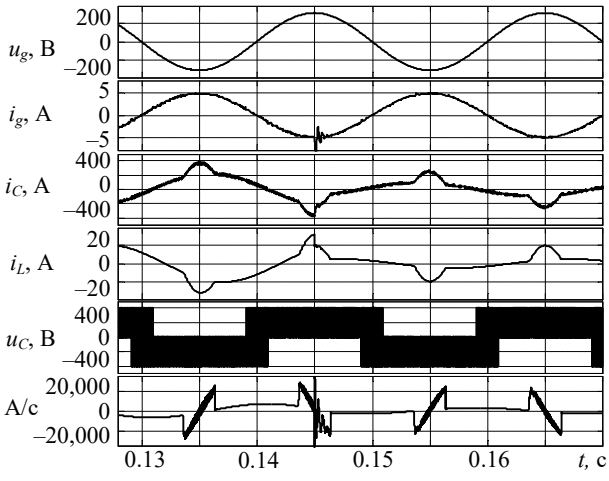

Fig. 8. u_g, u_C, i_g, i_C, i_L and $\mathrm{d}i_C^*/\mathrm{d}t$ oscillograms when the load changes

So, in the presence of the 3rd and 5th harmonics of DG voltage, the value of THDi_g≤5 % is maintained in the range of DG current values, starting with I_{gm}=5 A and above. Fig. 9, shows the oscillograms in the presence of the 3rd and 5th harmonics and Fig. 10 in the presence of all harmonics. Also, in Table 2 for the same values of current, THDi_{g1} values are presented in the absence of compensation.

Table 2

THDi_g values

n	I_{gm}^*, A	THDi_g, %	THDi_{g1}, %
3	3	4.25	15.3
5	4	4.8	22.7
3+5	5	3.9	20.3
7	5.5	4.75	19.2
3+5+7	6	4.98	24.1
9	3.5	4.68	12. 3
11	8	5	14.7
13	9.5	4.9	12.6
17	10.5	4.8	10.1
all	16.5	4.98	15

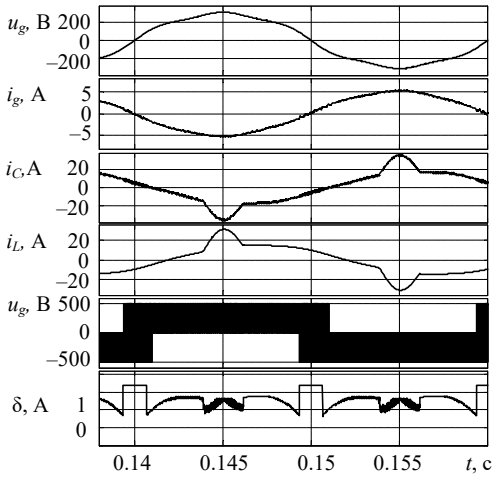

Fig. 9. u_g, u_C, i_g, i_C, i_L, δ oscillograms in the presence of the 3rd, 5th harmonics u_g

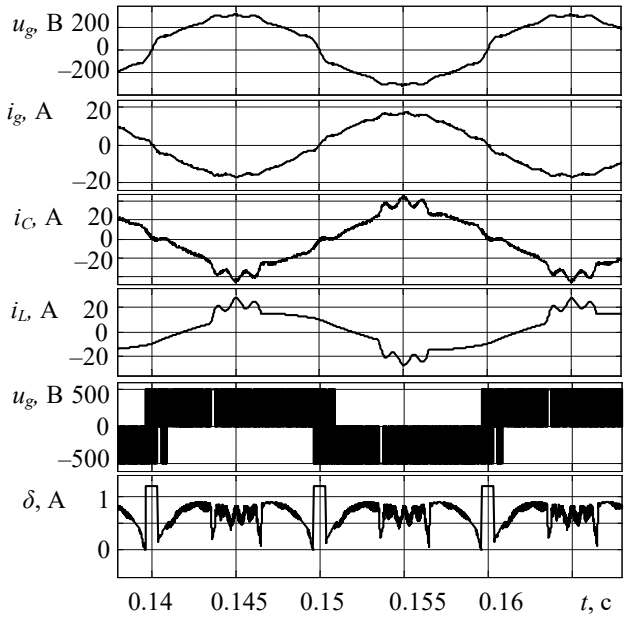

Fig. 10. u_g, u_C, i_g, i_C, i_L oscillograms in the presence of the 3rd, 5th, ...17th harmonics u_g

Increasing the voltage at the VSI input to U=500 V leads to an increase in power losses in the VSI switches compared to U=405 V. So, at $I^*_{gm}=3$ A, an increase in power losses is 18 % (efficiency 0.971, THDi_g=4.22 %), at I^*_{gm} =10 A – 17 % (efficiency 0.971, THDi_g=1.45 %), at $I^*_{gm}=17.8$ A – 15 % (efficiency 0.97, THDi_g=0.8 %).

5. Discussion of the research results on the improvement of CCL of EPS multifunctional grid inverter

Providing the value THDi_g≤5 % without increasing the filter and switching frequency of the switches without the deterioration of VSI efficiency is possible:

– for a linear reactor due to stabilization and reduction of the switching frequency f_S of the VSI switches. This is achieved by adjusting the reference value of RCC deviation according to the mains voltage, taking into account the derivative of the VSI current reference signal. With a constant f_S value, the advantage of RCC compared to PWM is that there is no error in the process of current formation;

– for a non-linear reactor, the formation of the reference value of RCC deviation is carried out taking into account the VSI current amplitude. In the zone of small current amplitudes, when L=const, the current deviation is formed as for a linear reactor. With increasing current amplitude, the f_s value is equalized in time. In the areas in the zone of values close to the amplitude, the frequency decreases by increasing the deviation reference; when the current decreases, the frequency increases by decreasing the deviation reference;

– by the introduction of communication for the filter capacitor current in the channel for the formation of the VSI current reference. This will make it possible to compensate for higher harmonics of low order, which are caused by the non-sinusoidal DG voltage.

This work is an extension of [16], where RCC for the combined modulation of the VSI voltage and a constant value of the reference deviation of the RCC is proposed to use. In this case, ensuring the harmonic current composition is possible at a sufficiently high f_S. A feature of the proposed solutions is the purposeful regulation of the PPT deviation reference with a decrease in f_S. At the same time, the possibilities of using a nonlinear reactor and VSI operation at a non-sinusoidal DG voltage were taken into account.

Some restrictions on the application of the results of the work are related to the fact that:

– the voltage value at the VSI input at a non-sinusoidal DG voltage was obtained for a specific rate of changes in the current of the nonlinear load – a rectifier with an output capacitive filter;

– a model with a certain dependence L (I_C) was used as a nonlinear reactor, when at a current I_C≈(0–0.5 I_{CMAX}), the value L=0.0042 H and then decreases by 2.65 times.

Research on the use of a nonlinear reactor at this stage of the work is evaluative. The goal is to identify the possibility of compensating the increase in the rate of changes in the VSI current with a decrease in L by changing the deviation of the RCC. This will limit and equalize the f_S values for the period of the mains voltage. The problem is that a decrease in inductance occurs at high currents of the VSI. In this case, the "splash" does not significantly affect the quality of the current, but the switching energy loss increases. This leads to an unacceptable decrease in inverter efficiency.

The development of this work is associated with the establishment of dependences for the deviation of RCC when using a nonlinear reactor in accordance with the instantaneous current value. The issues of ensuring the required indicators of grid VSI at non-sinusoidal DG voltage are subject to in-depth research. The problem is that the standard defines the value THDu_g≤8 % in the presence of voltage harmonics up to the 40th. The possibilities of their compensation depend on the order of harmonics.

6. Conclusions

1. The mechanism of VSI current formation and occurrence of "splash" of the grid current is investigated. The dependence of the given deviation for RCC is obtained, the use of which with a linear reactor provides an almost constant switching frequency of the VSI switches. To suppress the "splash", it is proposed to use dynamic compensation for the derivative of the VSI current in the process of forming the set value of RCC deviation. For a nonlinear reactor, with an increase in the amplitude of the VSI current as a result of an increase in the switching frequency of the switches, dynamic compensation is ineffective. The appearance of "splashes" in this case is associated with a sharp change in inductance. The suppression of "splashes" is achieved by a corresponding change in the reference deviation value of the RCC.

2. It is shown that for the non-sinusoidal DG voltage for ensuring the quality of the grid current, it is necessary to take into account the increase in the change rate of the reference current, which causes the corresponding voltage increase at the VSI input. Also, it is necessary to exclude the influence of the current harmonics of the filter capacitor at PCC. Full or partial compensation of these harmonics is possible with the introduction of capacitor current coupling into the channel of VSI current formation with the corresponding values of capacitor capacitance and resistance of the series-connected resistor.

3. The structure of the VSI control system using a relay current controller with the combined modulation of the output voltage is developed. In this case, the reference devi-

ation for the relay controller is regulated in accordance with the reference of amplitude and derivative of the VSI current. This allows getting THD≤5 % for the PCC in almost the entire range of the current. In combination with a modified key switching algorithm, this provides efficiency of at least 97 % when taking into account power losses in the VSI switches.

4. A detailed mathematical model for a PC is developed for a comprehensive study of the operation of the system "DG – grid inverter – load", including the determination of power losses in the switches. The load model together with the linear RL load contains a nonlinear load – a rectifier with a given value of the rate of changes in the input current. It is possible to obtain the required harmonic composition of the DG voltage, use a linear or non-linear reactor. This allowed carrying out studies with non-sinusoidal DG voltage and using a nonlinear output reactor. The results were used to clarify the voltage value at the VSI input and set the deviation of the relay controller.

Acknowledgments

This material is based upon the works supported by the Ministry of education and science of Ukraine under the Grants: 0117U000605 "Principles of creation of energy-efficient converters of combined power supply systems with renewable sources" and 0118U000232 "Development of a system of energy-efficient management of micro-energy grids of local objects with traditional and renewable sources".

References

1. Ko, S.-H., Lee, S.-R., Dehbonei, H., Nayar, C. V. (2006). A Grid-Connected Photovoltaic System with Direct Coupled Power Quality Control. IECON 2006 - 32nd Annual Conference on IEEE Industrial Electronics. doi: https://doi.org/10.1109/iecon.2006.347757
2. Zeng, Z., Yang, H., Zhao, R., Cheng, C. (2013). Topologies and control strategies of multi-functional grid-connected inverters for power quality enhancement: A comprehensive review. Renewable and Sustainable Energy Reviews, 24, 223–270. doi: https://doi.org/10.1016/j.rser.2013.03.033
3. Shavelkin, A. A. (2018). Structures of single-phase convertors units for combined electrical supply systems with photoelectric solar panels. Tekhnichna Elektrodynamika, 2, 39–46. doi: https://doi.org/10.15407/techned2018.02.039
4. Shavelkin, A., Shvedchykova, I. (2018). Multifunctional converter for single-phase combined power supply systems for local objects with a photovoltaic solar battery. Tekhnichna Elektrodynamika, 5, 92–95. doi: https://doi.org/10.15407/techned2018.05.092
5. Vigneysh, T., Kumarappan, N. (2017). Grid interconnection of renewable energy sources using multifunctional grid-interactive converters: A fuzzy logic based approach. Electric Power Systems Research, 151, 359–368. doi: https://doi.org/10.1016/j.epsr.2017.06.010
6. Brochures. ABB solar inverters. Available at: https://new.abb.com/power-converters-inverters/solar
7. 519-1992 - IEEE Recommended Practices and Requirements for Harmonic Control in Electrical Power Systems. doi: https://doi.org/10.1109/ieeestd.1993.114370
8. 1547-2018 - IEEE Standard for Interconnection and Interoperability of Distributed Energy Resources with Associated Electric Power Systems Interfaces. doi: https://doi.org/10.1109/ieeestd.2018.8332112
9. Da Silva, S. A. O., Sampaio, L. P., Campanhol, L. B. G. (2014). Single-phase grid-tied photovoltaic system with boost converter and active filtering. 2014 IEEE 23rd International Symposium on Industrial Electronics (ISIE). doi: https://doi.org/10.1109/isie.2014.6865013
10. Martins, D. C., de Souza, K. C. A. (2008). A Single-Phase Grid-Connected PV System With Active Power Filter. International Journal of Circuits, Systems and Signal Processing, 2 (1), 50–55.
11. Vaquero, J., Vázquez, N., Soriano, I., Vázquez, J. (2018). Grid-Connected Photovoltaic System with Active Power Filtering Functionality. International Journal of Photoenergy, 2018, 1–9. doi: https://doi.org/10.1155/2018/2140797
12. Mendez, I., Vazquez, N., Vaquero, J., Vazquez, J., Hernandez, C., Lopez, H. (2015). Multifunctional grid-connected photovoltaic-system controlled by sliding mode. IECON 2015 - 41st Annual Conference of the IEEE Industrial Electronics Society. doi: https://doi.org/10.1109/iecon.2015.7392286
13. Shavelkin, A. A. (2019). Improvement of the structure for the current control loop with the use of PWM for the grid inverter of the combined power supply system. Tekhnichna Elektrodynamika, 3, 37–45. doi: https://doi.org/10.15407/techned2019.03.037
14. Ma, T.-T. (2012). Power Quality Enhancement in Micro-grids Using Multifunctional DG Inverters. Proceedings of the International MultiConference of Engineers and Computer Scientists. Vol. II, IMECS 2012. Hong Kong, 996–1001.
15. Mao, H., Yang, X., Chen, Z., Wang, Z. (2012). A Hysteresis Current Controller for Single-Phase Three-Level Voltage Source Inverters. IEEE Transactions on Power Electronics, 27 (7), 3330–3339. doi: https://doi.org/10.1109/tpel.2011.2181419
16. Shavolkin, O., Shvedchykova, I. (2018). Forming of Current of the Single-Phase Grid Inverter of Local Combined Power Supply System with a Photovoltaic Solar Battery. 2018 IEEE 3rd International Conference on Intelligent Energy and Power Systems (IEPS). doi: https://doi.org/10.1109/ieps.2018.8559540
17. Wu, T.-F., Nien, H.-S., Shen, C.-L., Chen, T.-M. (2005). A Single-Phase Inverter System for PV Power Injection and Active Power Filtering With Nonlinear Inductor Consideration. IEEE Transactions on Industry Applications, 41 (4), 1075–1083. doi: https://doi.org/10.1109/tia.2005.851035
18. Machado, S. M., Da Silva, N. (2016). Stability and Harmonic Rejection Analysis of Single-Phase Grid-Connected Inverter Intended for Renewable Energy Systems Considering Distorted Grid Conditions. 2016 CIGRE C4 International Colloquium on EMC, Lightning and Power Quality Considerations for Renewable Energy Systems. Available at: https://www.researchgate.net/publication/299524329
19. IEEE Std EN 50160:2010. Voltage characteristics of electricity supplied by public electricity networks.
20. IGBT Modules. SEMIKRON. Available at: https://www.semikron.com/products/product-classes/igbt-modules.html
21. Shavolkin O. O., Stanovskyiy E. Yu., Pidhainyi M. O. (2019). Modeling of the combined electricpower system of a local object with multifunctionalconverter unit of photovoltaic battery. Visnyk Kyivskoho natsionalnoho universytetu tekhnolohii ta dyzainu, 4 (136), 20–33. doi: https://doi.org/10.30857/1813-6796.2019.4.2